Dinuclear nickel(II) complexes with ONO-pincer and coordinated aquo ligands as a robust homogeneous water oxidation catalyst

A. Khurshid,[a] M. N. Zafar,[a]★ K. Javed,[b] N. Iqbal,[c] and M. N. Arshad[d]

[a]*Department of Chemistry, Quaid-i-Azam University, Islamabad 45320, Pakistan. E-mail: mnzafar@qau.edu.pk*
[b]*Department of Chemistry, University of Gujrat, Gujrat, Pakistan*
[c]*U. S.-Pakistan Centre for Advanced Studies in Energy, National University of Sciences and Technology, Sector H-12, Islamabad 44000, Pakistan*
[d]*Chemistry Department, Faculty of Science, King Abdul Aziz University, Jeddah 21589, Saudi Arabia*

A nickel(II) complex with the newly synthesized dicarboxamide ligand $[H_2L_{BZ}][(CF_3SO_3)Cl]$ was explored as a water oxidation catalysis. All the synthesized compounds were characterized by IR and NMR spectroscopy, thermogravimetry, and single-crystal XRD analysis. The superior kinetics of the water oxidation reaction in the presence of the Ni^{II} catalyst was shown by an enhanced current of 4535 μA (pH 8) or 8900 μA (pH 10) at an overpotential of 186 mV in a cyclic voltammogram. Controlled potential electrolysis demonstrated that the catalyst was stable during the water oxidation experiment. These results are akin to those for other reported nickel catalysts.

Key words: catalytic water oxidation, dicarboxamide ligands, nickel(II) complex, homogeneous catalysis, pincer ligands.

One of the most challenging tasks for researchers in the 21st century is the production of green and sustainable energy from renewable sources.[1—5] Water is the only cheap and abundantly available source of electrons and protons for natural aerobic photosynthesis as well as artificial photosynthesis. The water oxidation is an attractive research area since it involves studies of a complicated mechanism of the rearrangement of different bonds like O—O bond formation and multiple proton-coupled electron transfer resulting in O_2 evolution with the generation of four electrons and four protons[6] as shown in Eq. (1).

$$2\,H_2O \longrightarrow O_2 + 4\,H^+ + 4e^- . \qquad (1)$$

Utilization of water as a source of hydrogen and oxygen in energy production needs highly efficient water oxidation catalysts (WOCs).[7]

Transition metals capable of transforming into high oxidation states during the water oxidation catalytic cycle make them an ideal choice to serve as a central atom of the main core of the catalyst. Among transition metals, a Ni catalyst is a superior choice for the construction of molecular systems for water oxidation because cyclic voltammetry (CV) of the complex shows no crossover, the catalytic current and concentration exhibit a direct relationship, no catalytic response is given by free Ni ions at acidic or neutral pH, no current enhancement occurs during repeating CV cycles, and no current is observed at the working electrode at the end of electrolysis.[8—10] Thus, an iron/nickel coordination polymer with carboxylate ligands for the water oxidation reaction was recently developed.[11] This polymer demonstrated good catalytic activity with an onset potential E^0 = 1.4 V. Spiccia and co-workers[9] presented nickel bound to oxygen donors like $[Ni(OH_2)_6]^{2+}$, $[Ni(tacn)_2]^{2+}$ (tacn is 1,4,7-triazacyclononane), $[Ni(tacn)(OH_2)_3]^{2+}$, and $[Ni(cyclen)(OH_2)_2]^{2+}$ (cyclen is 1,4,7,10-tetraazacyclododecane) for oxidation of water at pH 9.2. Water oxidation catalysis at neutral pH was carried out by Han *et al.*[10] using the cationic nickel(II) complex with *meso*-tetrakis(4-*N*-methylpyridyl)porphyrin at pH 10.8.

In homogeneous water oxidation catalysis, the design of catalyst plays a crucial role. Extremely active catalysts contain coordinated water molecules,[10—14] such as the aquo nickel complex $[Ni(mep)(H_2O)_2](ClO_4)_2$,[12] Mayer's blue dimer,[13] a catalyst with *cis* aqua, *cis* labile sites,[10] or a dimer with two water molecules coordinated in a similar manner.[14] These complexes have more intricate redox properties due to facilitated gain or loss of protons.[15]

Published in Russian in *Izvestiya Akademii Nauk. Seriya Khimicheskaya,* No. 11, pp. 2121—2128, November, 2020.
1066-5285/20/6911-2121

Similarly, using ligands that predominantly involve oxygen atoms in the first coordination sphere, rather than more readily oxidizable nitrogens slows down the rate of undesired catalyst degradation. Hydrogen bonding also boosts the kinetics of the water oxidation reaction.[16–18]

Basicity of ligand atoms speeds up proton transfer that may lower the overpotential needed for water oxidation. Thummel's group used ligands capable of hydrogen bonding and proton transfer for excellent WOCs.[19] In the same way, introducing Brønsted base, *i.e.* the interface of the OH^- ions with high-valent atoms, can facilitate the proton-coupled electron transfer and has remarkable effects on the reaction mechanism.[20,21] These features motivated researchers to develop transition metal WOCs based on O donor ligands.

In order to gain high oxidation states of transition metals during water oxidation catalytic cycle, the resonance of electrons at the metal center and ligand is an attractive concept. Redox-active ligands based on pyridine-based pincers as well as strongly electron donating carboxylates and oxalates were found very active for water oxidation catalysis,[19,22,23] *e.g.* dicarboxylate-ligated catalysts described by Sun's[24] and Llobet's[25,26] groups (the corresponding ligands are shown below).

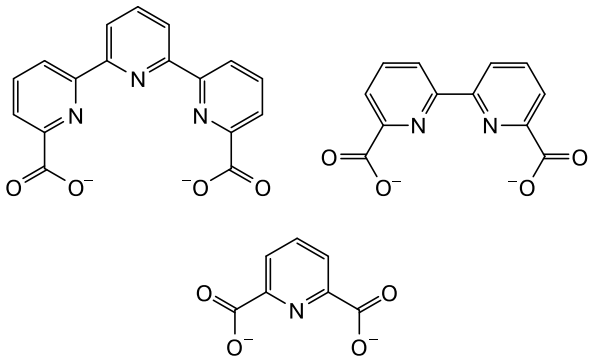

Therefore, a ligand with these functionalities can present unforeseeable challenges and thus used in this work. Herein, we reported the synthesis and characterization of the new $[H_2L_{BZ}][(CF_3SO_3)Cl]$ proligand used for the generation of an ONO-pincer ligand. We also prepared a nickel(II) dimer with one nickel atom coordinated with pyridine possessing a pendant dicarboxamide pincer ligand and the other nickel atom-coordinated water. This complex showed excellent catalytic activity towards water oxidation at basic pH values.

Results and Discussion

The $[H_2L_{BZ}][(CF_3SO_3)Cl]$ proligand was synthesized in two steps by (*i*) reacting pyridine-2,6-dicarbonyl dichloride with 4-aminopyridine to give *N*,*N*′-bis(2-pyridinyl)-2,6-pyridinedicarboxamide (compound **1**) and (*ii*) subsequent benzylation of pendant pyridine arms to form target proligand **2**. The IR spectrum of proligand **2** showed a broad N—H stretching band at 3431 cm^{-1}. A sharp C=O band appeared at 1691 cm^{-1}. Stretching frequencies for aromatic C—H bonds occurred at 3063 cm^{-1}. The weak aliphatic stretching vibrations for a sp^3 carbon atom at 2993 cm^{-1} revealed the presence of the benzyl group. Breathing or skeleton vibrations of aromatic rings appeared at their characteristic regions.[27] The ^1H NMR spectrum of proligand **2** showed a NH proton singlet signal at δ 13.19 and proton signals of the aromatic ring at δ 9.14—7.41.

Single-crystal XRD supported the suggested structure of proligand **2** (Fig. 1, *a*). Selected bond lengths (*d*) and bond angles (ω) are given in Table 1. These values matched well with the specified ranges given in the literature.[28] Importantly, the crystal structure of proligand **2** clearly confirms the successful benzylation of pendant pyridines of *N*,*N*′-bis(2-pyridinyl)-2,6-pyridinedicarboxamide (**1**). Figure 1, *b* illustrates the packing and hydrogen bonding in $[H_2L_{BZ}][(CF_3SO_3)Cl]$.

The complexation of proligand **2** with Ni^{II} was carried out by substitution of dimethoxyethane (DME) and chloride anions from $[Ni(DME)_2Cl_2]$. During the complexation reaction, the C—N bond of carboxamide in the $[H_2L_{BZ}][(CF_3SO_3)Cl]$ proligand (**2**) was hydrolyzed in the presence of 1,8-diazabicyclo[5.4.0]undec-7-ene (DBU) *via* base-catalyzed hydrolysis.[29–33] The general hydrolysis reaction is shown in Scheme 1.

Scheme 1

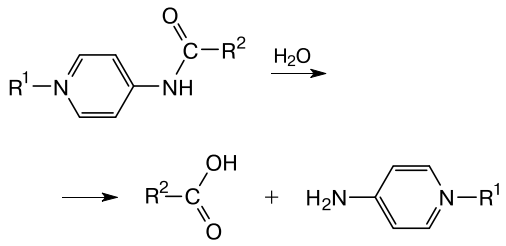

2,6-Pyridinedicarboxylic acid was further deprotonated to yield the dianionic ONO-pincer ligand that acted as a tridentate ligand for Ni^{II}. In the dimer, the Ni^{II} atom is

Table 1. Selected bond lengths (*d*) and bond angles (ω) of the proligand $[H_2L_{BZ}][(CF_3SO_3)Cl]$ (**2**)

Bond	*d*/Å	Angle	ω/deg
C(1)—N(1)	1.334(2)	N(1)—C(1)—C(2)	123.6(2)
C(5)—N(1)	1.333(2)	N(1)—C(1)—C(6)	117.8(2)
C(6)—O(1)	1.208(2)	O(1)—C(6)—N(2)	124.4(2)
C(6)—N(2)	1.367(3)	O(1)—C(6)—C(1)	121.3(2)
C(12)—N(3)	1.496(3)	N(2)—C(6)—C(1)	114.3(2)
C(19)—O(2)	1.216(2)	N(2)—C(7)—C(11)	117.8(2)
C(19)—N(4)	1.375(3)	C(19)—N(4)—C(20)	126.9(2)

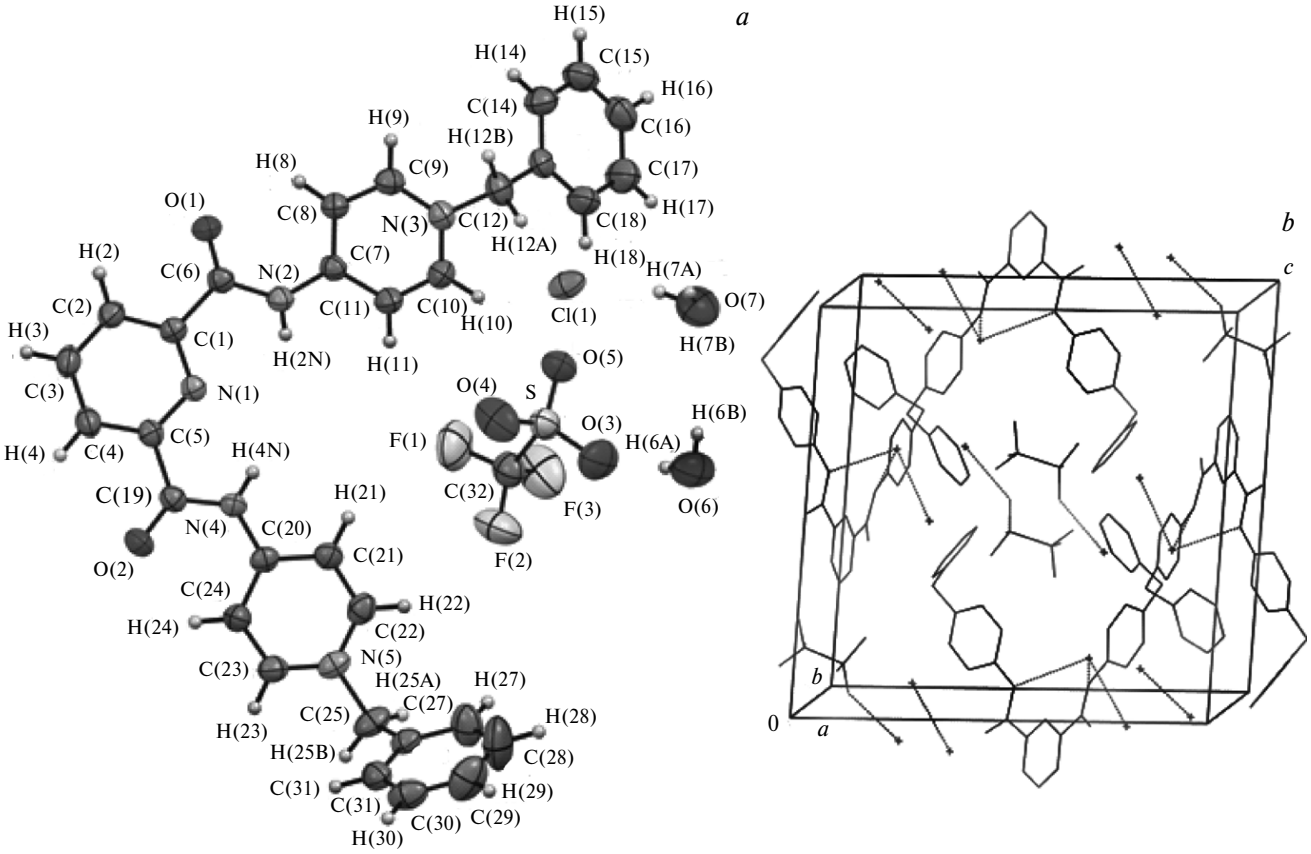

Fig. 1. ORTEP diagram (*a*) and the crystal packing and hydrogen bonding (*b*) of the proligand $[H_2L_{BZ}][(CF_3SO_3)Cl]$ (**2**).

surrounded by two negatively charged ligands, and the second negative charge is balanced by the second Ni^{II} atom that is surrounded by five coordinated aquo ligands.

The catalytic complex $[(NiL_2)(Ni(H_2O)_5)] \cdot 2H_2O$ (**3**) was fully characterized by IR and NMR spectroscopy, thermogravimetric analysis (TGA), and single-crystal XRD.

The IR spectrum of complex **3** showed peaks in their characteristic regions. A broad peak at 3357 cm^{-1} is due to ν(O—H) of coordinated water molecules. A weak aromatic C—H stretching occurred at 3035 cm^{-1}, while a sharp peak of the amide carbonyl group was observed at 1645 cm^{-1}. Sharp peaks at 519 and 557 cm^{-1} indicated the presence of Ni—O and Ni—N bonds, respectively.[34,35]

The ORTEP diagram of dinuclear nickel(II) complex **3** is shown in Fig. 2, *a*.

Complex **3** crystallizes in monoclinic space group $P2_1/c$. The coordination environment of the Ni(1) atom (NiN_6) is an octahedron formed by six nitrogen atoms of two chelating ligands. The geometry of the Ni(2) atom is also octahedral (NiO_6) and includes one oxygen atom of the amide group and five oxygen atoms of water molecules. Selected bond lengths and bond angles of nickel complex **3** are given in Table 2. All bond lengths and bond angles are in accordance with the literature values.[36] Hydrogen bonding and the packing diagram of complex **3** are shown in Fig. 2, *b*.

Thermal analysis revealed that the first inflection point observed at 350 °C corresponds to the melting point of complex **3**, while the second inflection point above 500 °C corresponds to decomposition of the metal complex into oxides (Fig. 3). The differential thermal analysis plot shows four endothermic and five exothermic peaks.

Catalysis of water oxidation by nickel(II) complex 3. The complex $[(NiL_2)(Ni(H_2O)_5)] \cdot 2H_2O$ (**3**) possesses essential structural characteristics of a good water oxidation catalyst.[24,25] First, the pendant carboxyl groups conjugated to the central redox-active pyridine ring make it a non-innocent ligand, which is an essential feature of a good ligand for WOC. The second salient feature of this dimer is the presence of water molecules coordinated to Ni^{II} that fits with the concept proposed by Mayer[15] of more active WOCs. These characteristics of complex **3** motivated us to study its catalytic activity towards the water oxidation reaction.

Cyclic voltammetry of a 1 m*M* solution of catalyst **3** was carried out at pH 8 and 10 in 0.1 *M* potassium phosphate buffer. Glassy carbon and Ag/AgCl electrodes were used as the working and reference electrodes, respectively.

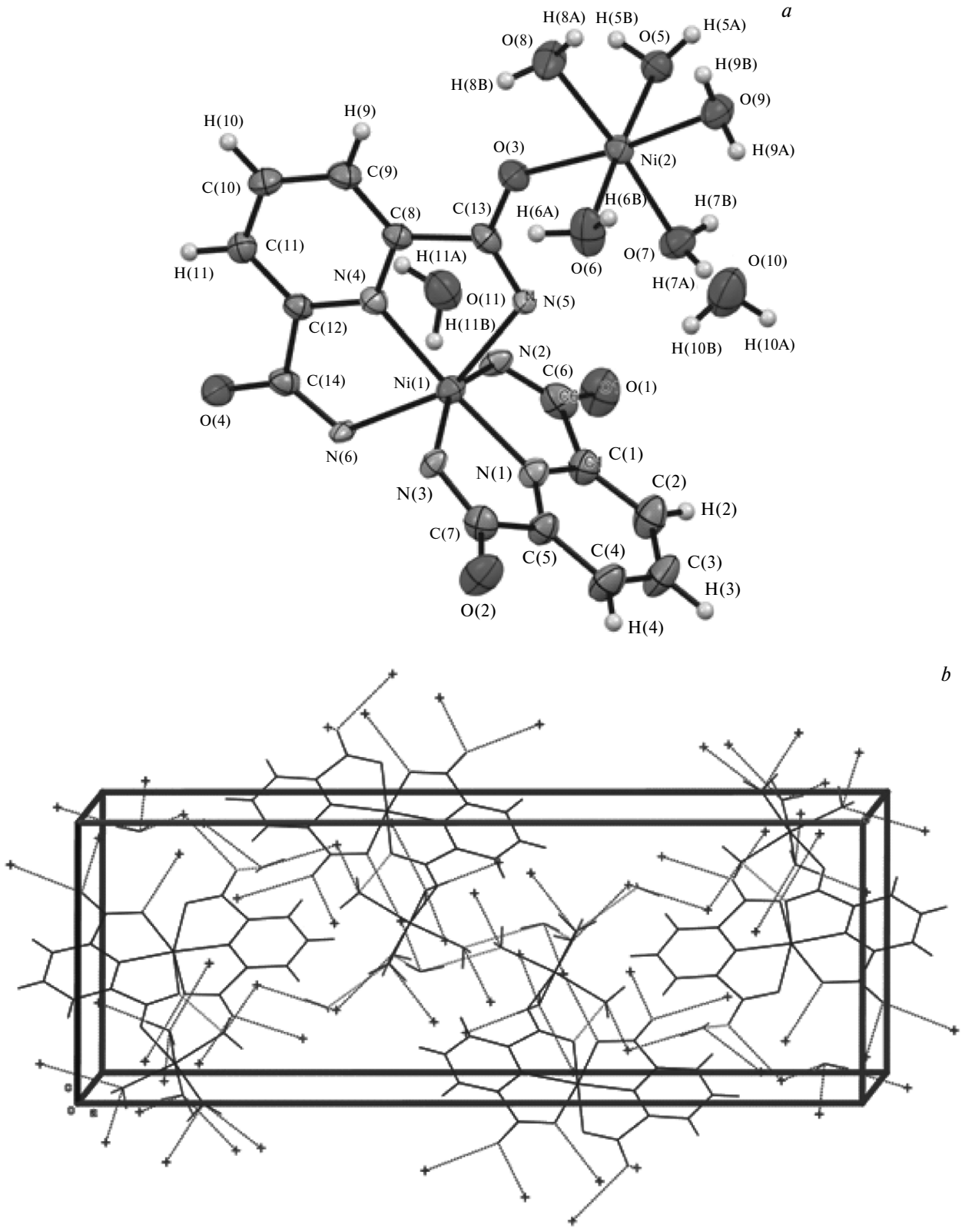

Fig. 2. ORTEP diagram (*a*) and the crystal packing and hydrogen bonding (*b*) of the nickel(II) complex $[(NiL_2)(Ni(H_2O)_5)]\cdot 2H_2O$ (**3**).

As the reaction proceeds, oxygen bubbles were found evolving around the anode. Cyclic voltammograms are shown in Figs 4, *a*—*c*. The addition of catalyst **3** significantly enhanced the peak current as compared to the blank

Table 2. Selected bond lengths (*d*) and bond angles (ω) of nickel(II) complex **3**

Bond	*d*/Å	Angle	ω/deg	Angle	ω/deg
C(1)—N(1)	1.329(03)	N(1)—C(1)—C(2)	121.4(02)	N(1)—Ni(1)—N(2)	174.9(08)
N(1)—Ni(1)	1.959(02)	N(1)—C(1)—C(6)	112.2(02)	N(1)—Ni(1)—O(2)	78.2(08)
N(2)—Ni(1)	1.969(02)	C(1)—N(1)—C(5)	121.5(02)	O(2)—Ni(1)—O(4)	155.1(07)
O(2)—Ni(1)	2.098(18)	C(1)—N(1)—Ni(1)	118.4(17)	N(1)—Ni(1)—O(8)	107.8(08)
O(4)—Ni(1)	2.156(17)	C(7)—O(4)—Ni(1)	113.9(16)	O(2)—Ni(1)—O(6)	95.3(08)
O(8)—Ni(1)	2.165(18)	C(13)—O(5)—Ni(2)	133.8(17)	O(5)—Ni(2)—O(9)	172.9(08)

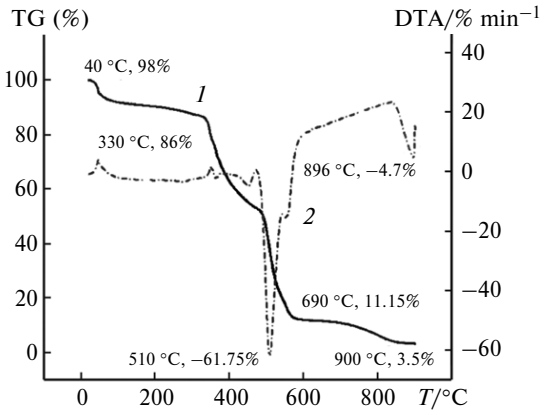

Fig. 3. TG (*1*) and DTA (*2*) curves for the nickel(II) complex $[(NiL_2)(Ni(H_2O)_5)]\cdot 2H_2O$ (**3**).

buffer solution at both selected pH values. It can be seen that the higher the pH value the larger the area of voltammogram, which reflects the faster kinetics of the water oxidation reaction. When the homogeneous solution of catalyst **3** was scanned in the range from +0.2 to +1.7 V at pH 8, the CV curve shows an intense irreversible peak current of 4535 μA at 1.57 V (see Fig. 4, *a*). Figures 4, *b*,*c* show the effect of different scan rates on peak currents at two different selected pH values. It was found that the onset potential for water oxidation in the presence of complex **3** is *ca*. 1.18 V *vs* Ag/AgCl with an overpotential of 186 mV, which is in agreement with the best catalysts for homogeneous water oxidation reactions (300—600 mV).[37]

Bulk electrolysis (controlled potential electrolysis) was performed at η = 1.6 V to check the stability of the catalyst.

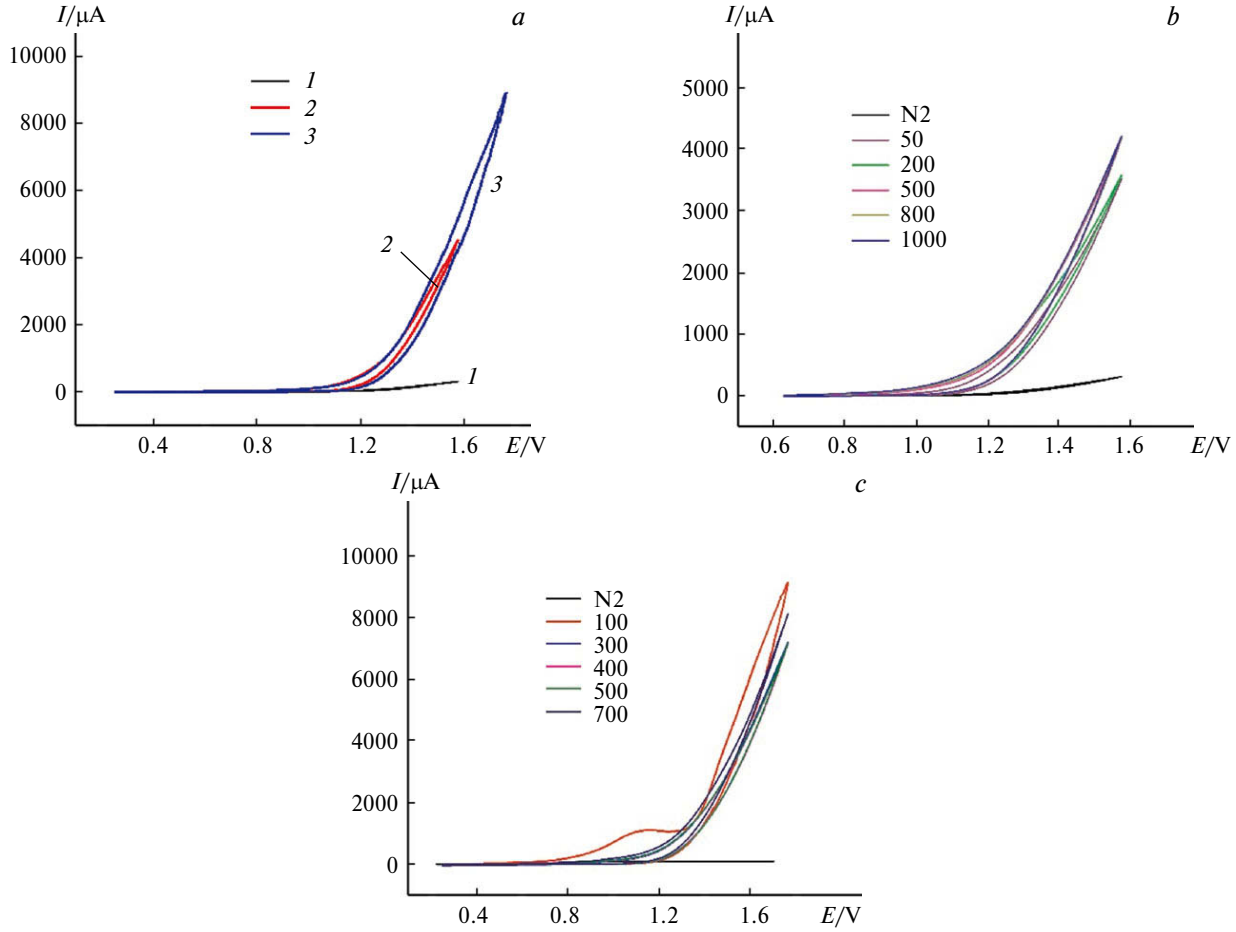

Fig. 4. CV curves of complex **3** in 0.1 *M* K_3PO_4 buffer at different pH values (*a*) and at scan rates *v* = 10—1000 (*b*) and 100—750 mV s^{-1} (*c*); (*a*) the initial buffer in the absence (*1*) and in the presence of nickel complex **3** ($C = 1\cdot 10^{-3}$ mol L^{-1}) at pH 8 (*2*) and 10 (*3*). *Note*. Fig. 4 is available in full color on the web page of the journal (https://link.springer.com/journal/volumesAndIssues/11172).

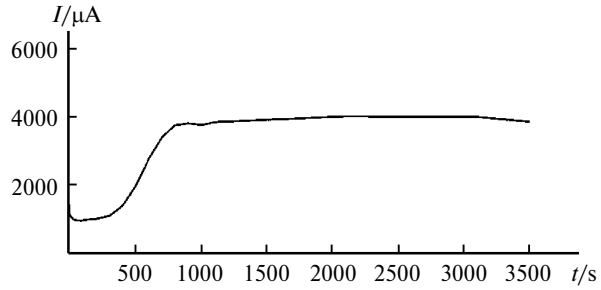

Fig. 5. Controlled potentiometry of the complex $[Ni_2(L)_2(H_2O)_5]\cdot 2H_2O$ (**3**).

The time *vs.* current curve (Fig. 5) shows no significant current fluctuations within 1 h. This clearly reveals that there is no degradation of electro-active species during the controlled potential electrolysis experiment. However, during initial 500 s the current was low but after *ca.* 800 s, it increased. This can be attributed to the time required to establish an equilibrium in the catalyst diffusion process.

Table 3 summarizes the electrochemical parameters of selected nickel catalysts in the water oxidation reaction.

In summary, a new proligand $[H_2L_{BZ}][(CF_3SO_3)Cl]$ (**2**) was successfully synthesized by treating pyridine-2,6-dicarbonyl dichloride with 4-aminopyridine followed by benzylation of the pendant pyridine arms. The redox-active Ni^{II} complex was synthesized by the reaction of proligand **2** with $[Ni(DME)_2Cl_2]$ in the presence of non-nucleophilic base. *In situ* base-catalyzed hydrolysis of the carboxamide group of proligand **2** yielded a tridentate dicationic ONO-pincer ligand to give the nickel(II) complex $[(NiL_2)(Ni(H_2O)_5)]\cdot 2H_2O$ (**3**). The single-crystal XRD analysis demonstrated that complex **3** is a dimer with one Ni^{II} atom surrounded by two ONO-pincer ligands (L) and another Ni^{II} atom is surrounded by five coordinated water molecules and the oxygen atom of the ligand. The synthesized Ni^{II} complex **3** immensely increased the kinetics of the water oxidation reaction. The increased rate of the water oxidation reaction was shown by an enhanced current, *i.e.*, 4535 μA (pH 8) and 8900 μA (pH 10) at an overpotential of 186 mV. Controlled potential electrolysis revealed the robustness of the catalyst for the water oxidation reaction.

Experimental

Unless otherwise specified, all chemical reactions were carried out under an inert atmosphere. All solvents and chemicals of analytical grade were purchased from Sigma. Solvents were dried prior to use. Single-crystal X-ray analysis was performed using an Agilent Super Nova diffractometer (Agilent Technologies), λ(Mo-Kα) = 0.71073 Å, graphite monochromator, ω scan mode (University of King Abdul Aziz, KSA). Single crystals of the proligand $[H_2L_{BZ}][(CF_3SO_3)Cl]$ (**2**) were grown as follows: proligand **2** was dissolved in methanol containing silver triflate, silver chloride that formed was filtered off, and the solution was allowed to slowly evaporate. Crystals of complex **3** suitable for single-crystal XRD were obtained by slow evaporation of its solution in distilled water. The structures were solved using the SHELXL-97 software. Data collection, indexing, and processing were carried out using the CrystalAlisPro software package. Crystallography data for compounds **2** and **3** are given in Tables 1 and 2. The IR spectra were recorded using a Perkin Elmer Spectrum 400 FT-IR spectrometer in the range of 4000—400 cm^{-1} as KBr pellets. The NMR spectra were measured at 300 K using a Bruker Avance spectrometer at 300 MHz (^1H) and 75 MHz (^{13}C) using Me_4Si as the reference for ^1H NMR spectra. The carbon signal of DMSO-d_6 (δ 39.43) was used as the reference for ^{13}C NMR spectra. Elemental analysis for C, H, and N was carried out on a Thermo Scientific Flash 2000 Elemental Analyzer. Thermogravimetric analysis was performed on a DTG-60H instrument (Shimadzu, Japan). The TG and DTA analyses (see Fig. 3) were carried out under a nitrogen flow (50 mL min^{-1}) in the temperature range of 20—900 °C. Electrocatalytic studies (cyclic voltammetry and controlled potential electrolysis) were performed using a CHI760 electrochemical workstation (CH Instruments, Inc.). A cell with a three-electrode system (7 mm^2 glassy carbon working electrode, Pt mesh counter electrode, and Ag/AgCl reference electrode) was used for the analyses. Electrochemical studies were carried out using 0.1 *M* potassium phosphate buffer as the electrolyte. A homogeneous solution of catalyst **3** was scanned in the range from +0.2 to +1.7 V at a scan rate of 100 mV s^{-1}.

Synthesis of *N*,*N*′-bis(pyridin-2-yl)-2,6-pyridnedicarboxamide (1). A 100-mL two-neck round-bottom flask was charged with pyridine-2,6-dicarbonyl dichloride (2.04 g, 10.00 mmol, 1.00 eq.)

Table 3. Comparison of the catalytic parameters of the complex $[(NiL_2)(Ni(H_2O)_5)]\cdot 2H_2O$ (**3**) with other water oxidation electrocatalysts

Complex	Electrolyte	E/V	E^0/V	η/mV	pH	I/mA	Ref.
$[(NiL_2)(Ni(H_2O)_5)]\cdot 2H_2O$	0.1 *M* K_3PO_4	1.57	1.18 (*vs.* Ag/AgCl)	186	8.0	4535	Present work
$[(NiL_2)(Ni(H_2O)_5)]\cdot 2H_2O$	0.1 *M* K_3PO_4	1.57	1.18 (*vs.* Ag/AgCl)	186	10.0	8900	Present work
$[Ni(meso\text{-}L')]^{2+}$	0.1 *M* Na_3PO_4	1.41	0.99 (*vs.* NHE)	170	7.0	≥770	38
$NiFe_2O_4$	0.05 *M* K_3PO_4	1.50	0.80 (*vs.* SCE)	430	8.0	>650	39
NiFe-DH	1 *M* KOH	1.40	0.90 (*vs.* RHE)	258	13.6	1420	40
NiFeP	1 *M* KOH	1.40	0.90 (*vs.* RHE)	258	13.6	6450	40

Note. L′ is 5,5,7,12,12,14-hexamethyl-1,4,8,11-tetraazacyclotetradecane, DH is double hydroxide, E is the peak potential, E^0 is the standard potential, η is the overpotential, NHE is the normal hydrogen electrode, SCE is the saturated calomel electrode, RHE is the reversible hydrogen electrode (the potential of RHE correlates to the pH value).

and dichloromethane (30 mL) under an inert atmosphere. Another 50-mL round-bottom flask was charged with 4-aminopyridine (1.88 g, 20.00 mmol, 2 eq.), triethylamine (4.20 mL, 5.79 g, 30.00 mmol), and dichloromethane (20 mL) and the obtained solution was transferred to the 100-mL flask. The resulting mixture was successively stirred at 0 °C for 5—10 min, at room temperature for 2 h, and then refluxed for 6 h. The reaction mixture was cooled to ambient temperature and the product obtained was filtered off. The dirty white precipitate was purified by washing with a saturated $NaHCO_3$ solution, distilled water, acetone, and diethyl ether until the pure white powder was obtained. This powder was dried to give 1.80 g (55%) of the pure title product.[41]

Synthesis of proligand $[H_2L_{BZ}][(CF_3SO_3)Cl]$ (2). Compound **1** (500 mg, 1.56 mmol, 1 equiv.), benzyl chloride (7.21 mL, 793 mg, 40 equiv.), and anhydrous MeCN (25 mL) were mixed in an evacuated 100-mL two-neck round-bottom flask. The reaction mixture was refluxed for 10 h. After cooling to room temperature, the white precipitate was collected by filtration and washed with acetone and diethyl ether to give 800 mg (90%) of the pure title product. Found (%): C, 55.97; H, 4.55; N, 10.20. $H_{27}N_5O_2CF_3O_3SCl \cdot 2(H_2O)$. Calculated (%): C, 55.92; H, 4.50; N, 10.17. ^{1}H NMR (300 MHz, DMSO-d_6), δ: 13.19 (s, 2 H, NH); 9.14 (d, 4 H, J = 7.2 Hz); 8.99 (d, 4 H, J = 7.2 Hz); 8.52 (m, 2 H); 8.41 (dd, 1 H, J = 8.7 Hz); 7.54 (m, 10 H); 5.77 (s, 4 H). ^{13}C NMR (75.0 MHz, DMSO-d^6), δ: 165.6, 152.9, 148. 145.5, 140.9, 135.2, 129.6, 128.9, 128.2, 117.4, 62.2. IR, ν/cm^{-1}: 3431, 3229, 3213, 3063, 2993, 1691, 1579, 1512, 1453, 1326, 1157, 1113, 732, 608.

Synthesis of complex $[(NiL_2)(Ni(H_2O)_5)] \cdot 2H_2O$ (3). A 50-mL two-neck round-bottom flask was charged with compound **2** (0.250 g, 0.436 mmol, 1 equiv.), $[Ni(DME)_2Cl_2]$ (0.108 g, 0.480 mmol, 1.1 equiv.), and anhydrous MeCN (25 mL) under an inert atmosphere. Then DBU (0.199 mL, 1.31 mmol, 3 equiv.) was added and the mixture was refluxed for 2 h. A yellow solid product precipitated from the reaction mixture. The reaction mixture was cooled to ambient temperature. The precipitate was filtered off, washed with acetone and diethyl ether, and dried to give 170 mg (63%) of complex **3**. Found (%): C, 33.74; H, 5.69; N, 4.31. $C_{14}H_{20}N_2Ni_2O_{15}$. Calculated (%): C, 33.79; H, 5.73; N, 4.29. IR, ν/cm^{-1}: 3357, 3035, 1645, 1609, 1583, 1342, 1200, 1163, 848, 771, 519.

The authors greatly acknowledge the Higher Education Commission (HEC) of the Pakistan for the research funding.

References

1. A. J. Bard, M. A. Fox, *Acc. Chem. Res.*, 1995, **28**, 141.
2. T. J. Meyer, *Acc. Chem. Res.*, 1989, **22**, 163.
3. J. Bockris, *Energy: the Solar-Hydrogen Alternative*, Halsted Press, New York, 1975.
4. J. D. Blakemore, R. H. Crabtree, G. W. Brudvig, *Chem. Rev.*, 2015, **115**, 12974.
5. H. B. Gray, *Nat. Chem.*, 2009, **1**, 112.
6. M. D. Kärkäs, T. Åkermark, H. Chen, J. Sun, B. Åkermark, *Angew. Chem., Int. Ed.*, 2013, **52**, 4189.
7. D. G. H. Hetterscheid, N. H. J. Reek, *Angew. Chem., Int. Ed.*, 2012, **51**, 9740.
8. G. Zhu, E. N. Glass, Ch. Zhao, H. Lv, J. W. Vickers, Y. V. Geletii, D. G. Musaev, J. Song, C. L. Hill, *Dalton Trans.*, 2012, **41**, 13043.
9. A. Singh, S. L. Y. Chang, R. K. Hocking, U. Bach, L. Spiccia, *Energy Environ. Sci.*, 2013, **6**, 579.
10. Y. Han, Y. Wu, W. Lai, R. Cao, *Inorg. Chem.*, 2015, **54**, 5604.
11. W. Li, F. Li, H. Yang, X. Wu, P. Zhang, Y. Shan, L. Sun, *Nat. Commun.*, 2019, **10**, 5074.
12. J.-W. Wang, X.-Q. Zhang, H.-H. Huang, T.-B. Lu, *ChemCatChem*, 2016, **8**, 3287.
13. S. W. Gersten, G. J. Samuels, T. J. Meyer, *J. Am. Chem. Soc.*, 1982, **104**, 4029.
14. J. A. Gilbert, D. Geselowitz, T. J. Meyer, *J. Am. Chem. Soc.*, 1986, **108**, 1493.
15. T. J. Meyer, *J. Electrochem. Soc.*, 1984, **131**, No. 7, 221C.
16. S. Maji, I. López, F. Bozoglian, J. Benet-Buchholz, A. Llobet, *Inorg. Chem.*, *2*013, **52**, 3591.
17. T. Privalov, B. Åkermark, L. Sun, *Chem. Eur. J.*, 2011, **17**, 8313.
18. D. C. Marelius, S. Bhagan, D. J. Charboneau, K. M. Schroeder, J. M. Kamdar, A. R. McGettigan, B. J. Freeman, C. E. Moore, A. L. Rheingold, A. L. Cooksy, *Eur. J. Inorg. Chem.*, 2014, **2014**, 676.
19. G. Zhang, R. Zong, H.-W. Tseng, R. P. Thummel, *Inorg. Chem.*, 2008, **47**, 990.
20. Z. Chen, J. J. Concepcion, X. Hu, W. Yang, P. G. Hoertz, T. J. Meyer, *Proc. Natl. Acad. Sci.*, 2010, **107**, 7225.
21. N. Song, J. J. Concepcion, R. A. Binstead, J. A. Rudd, A. K. Vannucci, C. J. Dares, M. K. Coggins, T. J. Meyer, *Proc. Natl. Acad. Sci.*, 2015, **112**, 4935.
22. L. Duan, A. Fischer, Yu. Xu, L. Sun, *J. Am. Chem. Soc.*, 2009, **131**, 10397.
23. P. J. Chirik, *Inorg. Chem.*, 2011, **50**, 9737.
24. L. Duan, F. Bozoglian, S. Mandal, B. Stewart, T. Privalov, A. Llobet, L. Sun, *Nat. Chem.*, 2012, **4**, 418.
25. P. Garrido-Barros, C. Gimbert-Suriñach, R. Matheu, X. Sala, A. Llobet, *Chem. Soc. Rev.*, 2017, **46**, 6088.
26. R. Matheu, M. Z. Ertem, J. Benet-Buchholz, E. Coronado, V. S. Batista, X. Sala, A. Llobet, *J. Am. Chem. Soc.*, 2015, **137**, 10786.
27. D. L. Pavia, G. M. Lampman, G. S. Kriz, J. A. Vyvyan, *Introduction to Spectroscopy*, Cengage Learning, Belmont, 2008.
28. H. Feilchenfeld, *J. Phys. Chem.*, 1959, **63**, 1346.
29. P. G. Gassman, P. K. G. Hodgson, R. J. Balchunis, *J. Am. Chem. Soc.*, 1976, **98**, 1275.
30. H. Slebocka-Tilk, A. J. Bennet, H. J. Hogg, R. S. Brown, *J. Am. Chem. Soc.*, 1991, **113**, 1288.
31. R. S. Brown, A. J. Bennet, H. Slebocka-Tilk, *Acc. Chem. Res.*, 1992, **25**, 481.
32. P. Deslongchamps, R. Barlet, R. J. Taillefer, *Can. J. Chem.*, 1980, **58**, 2167.
33. B. Galabov, D. Cheshmedzhieva, S. Ilieva, B. Hadjieva, *J. Phys. Chem. A.*, 2004, **108**, 11457.
34. A. S. Adekunle, J. A. O. Oyekunle, O. S. Oluwafem, A. O. Joshua, A. O. Makinde, A. O. Ogunfowokan, M. A. Eleruja, E. E. Ebenso, *Int. J. Electrochem. Sci.*, 2014, **9**, 3008.

35. K. C. Joshi, K. Dubey, *Die Pharmazie*, 1979, **34**, 801.
36. G. Azadi, Z. Zand, Y. Mousazade, R. Bagheri, J. Cui, Z. Song, R. Bikas, K. Wozniak, S. I. Allakhverdiev, M. M. Najafpour, *Int. J. Hydrog. Energy*, 2019, **44**, 2857.
37. C. A. Kent, J. J. Concepcion, C. J. Dares, D. A. Torelli, A. J. Rieth, A. S. Miller, P. G. Hoertz, T. J. Meyer, *J. Am. Chem. Soc.*, 2013, **135**, 8432.
38. M. Zhang, M.-T. Zhang, C. Hou, Z.-F. Ke, T.-Bu Lu, *Angew. Chem., Int. Ed.*, 2014, **53**, 13042.
39. D. Hong, Yu. Yamada, T. Nagatomi, Y. Takai, S. Fukuzumi, *J. Am. Chem. Soc.*, 2012, **134**, 19572.
40. H. Liang, A. N. Gandi, C. Xia, M. N. Hedhili, D. H. Anjum, U. Schwingenschlögl, H. N. Alshareef, N. Huzam, *ACS Energy Lett.*, 2017, **2**, 1035.
41. Z. Qin, M. C. Jennings, R. J. Puddephatt, *Inorg. Chem.*, 2003, **42**, 1956.

Received November 18, 2019;
accepted August 7, 2020